

PAPER • OPEN ACCESS

Energy-level alignment at strongly coupled organic–metal interfaces

To cite this article: Meng-Ting Chen *et al* 2019 *J. Phys.: Condens. Matter* **31** 194002

View the [article online](#) for updates and enhancements.








IOP | ebooks™

Bringing you innovative digital publishing with leading voices to create your essential collection of books in STEM research.

Start exploring the collection - download the first chapter of every title for free.

Energy-level alignment at strongly coupled organic–metal interfaces

Meng-Ting Chen¹, Oliver T Hofmann², Alexander Gerlach³, Benjamin Bröker⁴, Christoph Bürker³, Jens Niederhausen⁵, Takuya Hosokai⁶, Jörg Zegenhagen⁷, Antje Vollmer⁵, Ralph Rieger⁸, Klaus Müllen⁹, Frank Schreiber^{1,3}, Ingo Salzmann¹⁰, Norbert Koch^{1,4,5}, Egbert Zojer² and Steffen Duhm¹

¹ Institute of Functional Nano & Soft Materials (FUNSOM), Jiangsu Key Laboratory for Carbon-Based Functional Materials & Devices and Joint International Research Laboratory of Carbon-Based Functional Materials and Devices, Soochow University, 199 Ren-Ai Road, Suzhou 215123, People's Republic of China

² Institute of Solid State Physics, NAWI Graz, Graz University of Technology, Petersgasse 16, 8010 Graz, Austria

³ Institut für Angewandte Physik, Universität Tübingen, Auf der Morgenstelle 10, 72076 Tübingen, Germany

⁴ Institut für Physik, Humboldt-Universität zu Berlin & IRIS Adlershof, Brook-Taylor-Straße 6, 12489 Berlin, Germany

⁵ Helmholtz-Zentrum Berlin für Materialien und Energie GmbH, Albert-Einstein-Straße 15, 12489 Berlin, Germany

⁶ National Metrology Institute of Japan (NMIJ), National Institute of Advanced Industrial Science and Technology (AIST), Tsukuba, Ibaraki 305-8565, Japan

⁷ Diamond Light Source Ltd, Harwell Science and Innovation Campus, Didcot, Oxfordshire, OX11 0DE, United Kingdom

⁸ Max Planck Institut für Polymerforschung, Ackermannweg 10, 55128 Mainz, Germany

⁹ Institute of Physical Chemistry, Johannes Gutenberg University Mainz, Duesbergweg 10-14, 55128 Mainz, Germany

¹⁰ Department of Physics, Department of Chemistry & Biochemistry, Centre for Research in Molecular Modeling (CERMM) and Centre for NanoScience Research (CeNSR), Concordia University, 7141 Sherbrooke Street W., SP 265-20, Montreal, Quebec H4B 1R6, Canada

E-mail: duhm@suda.edu.cn

Received 30 October 2018, revised 14 January 2019

Accepted for publication 23 January 2019


Published 13 March 2019




Abstract

Energy-level alignment at organic–metal interfaces plays a crucial role for the performance of organic electronic devices. However, reliable models to predict energetics at strongly coupled interfaces are still lacking. We elucidate contact formation of 1,2,5,6,9,10-coronenehexone (COHON) to the (1 1 1)-surfaces of coinage metals by means of ultraviolet photoelectron spectroscopy, x-ray photoelectron spectroscopy, the x-ray standing wave technique, and density functional theory calculations. While for low COHON thicknesses, the work-functions of the systems vary considerably, for thicker organic films Fermi-level pinning leads to identical work functions of 5.2 eV for all COHON-covered metals irrespective of the pristine substrate work function and the interfacial interaction strength.

Keywords: organic–metal interface, energy-level alignment, photoelectron spectroscopy, x-ray standing waves, density functional theory

 Original content from this work may be used under the terms of the [Creative Commons Attribution 3.0 licence](https://creativecommons.org/licenses/by/3.0/). Any further distribution of this work must maintain attribution to the author(s) and the title of the work, journal citation and DOI.

 Supplementary material for this article is available [online](#)

(Some figures may appear in colour only in the online journal)

Introduction

Interfaces between conjugated organic molecules (COMs) and metals are of key importance in the field of organic electronics and the energy-level alignment is crucial for the performance of organic devices [1–5]. For weakly interacting interfaces, the energy-level alignment is well understood and—in a first approximation—determined by the work function of the metal (ϕ) and the ionization energy (IE) and electron affinity (EA) of the COM thin film [6–8]. IE and EA are often approximated by the onset energies of the frontier molecular orbital (highest occupied molecular orbital, HOMO, and lowest unoccupied molecular orbital, LUMO) with respect to the vacuum level (VL). By taking these positions and additionally their associated densities of states (DOS) into account, the coverage-dependent evolution of the VL relative to the Fermi-level (E_F) can be modeled with high precision using electrostatic models [9–12]. In contrast, at strongly coupled organic–metal interfaces often charge transfer complex (CTC) formation involving donation and backdonation of charges takes place. Despite tremendous research effort [13–37] a generalization of CTC formation is still lacking. Predicting interface dipoles (ΔVL) at organic–metal interfaces thus still requires an advanced level of quantum mechanical calculations [38–41].

The energy-level alignment of a COM on different substrates can be often categorized into two regimes [7, 12, 42, 43]: for low and high substrate work functions, the VL of the organic thin film is independent of the initial ϕ , i.e. these systems are Fermi-level pinned. On the other hand, for intermediate substrate work functions the energy-level alignment is vacuum-level controlled. Intriguingly, quite a few COMs are either VL or Fermi-level controlled on *all* (1 1 1)-surfaces of coinage metals, although these surfaces cover a work function range of almost 1 eV [44]. For example, for perylene [45], pentacene (PEN) [46] and their derivatives perylene-3,4,9,10-tetracarboxylic diimide (PTCDI) [29] and perfluoropentacene (PFP) [47–49], the substrate ϕ is still reflected in the VL positions of thin film multilayers on these substrates. The energy-level alignment at these interfaces is, thus, VL controlled. Conversely, for COMs like the perylene derivative 3,4,9,10-perylene-tetracarboxylic-dianhydride (PTCDA), the VL in multilayers becomes independent of the initial substrate ϕ , i.e. PTCDA is Fermi-level pinned on the (1 1 1)-surfaces of coinage metals [50] and substrates spanning a ϕ range from 3.3 eV to 5.3 eV [12]. Other examples are 2,3,5,6-tetrafluoro-7,7,8,8-tetracyanoquinodimethane (F4-TCNQ) [43] and 1,4,5,8,9,12-hexaazatriphenylene-hexacarbonitrile (HATCN) [51–54], which are Fermi-level pinned on various substrates. The EAs of F4-TCNQ and HATCN thin films (measured by inverse photoemission, IPES) are larger than 5 eV [53, 55, 56] and the Fermi-level becomes pinned in the proximity of the LUMO. The EA of PTCDA thin films, however, is only 4.10 eV

[57] and the Fermi-level is thus pinned relatively far from the LUMO (as well as the HOMO). This has been explained by the broadening of the DOS of the frontier PTCDA orbitals due to coupling with the substrates or by gap states [12].

Systems that undergo pinning on various substrates are preferred for electronic applications: for example, a several nm thin layer of HATCN on virtually any substrate provides a versatile hole injection electrode with a work function of ≈ 5.5 eV [51–54]. HATCN is indeed frequently used in organic optoelectronic devices [58–61]. For VL-controlled systems, however, energy-level engineering is less straightforward. Another factor hampering possible device application is molecular diffusion through organic layers, which has been observed for F4-TCNQ [62–68]. It has been suggested that larger molecules are less prone to diffusion than smaller molecules [62, 69].

In this contribution, we show that the energy levels of the relatively large molecule 1,2,5,6,9,10-coronenehexone (COHON) [70] are Fermi-level pinned on the (1 1 1)-surfaces of coinage metals. Moreover, following a multi-technique approach we get deep insight into the interaction of organic adsorbates with metal surfaces: in addition to ultraviolet photoelectron spectroscopy (UPS) that yields the energy-level alignment, we measured x-ray photoelectron spectroscopy (XPS) to access interfacial chemical interactions. We also employed the x-ray standing wave (XSW) technique [71, 72] for submonolayers of COHON on Cu(1 1 1) to determine element-specific vertical bonding distances at this interface with high precision. These experiments are complemented by density functional theory (DFT) calculations. In addition, we performed a full characterization of 1,2,6,7-pyrenetetron (PYTON) [73] on Cu(1 1 1) (see data in the supporting information, available online at stacks.iop.org/JPhysCM/31/194002/mmedia). For comparison, we measured the VLs of 6,13-pentacenequinone (P2O) and 5,7,12,14-pentacenetetrone (P4O) on the (1 1 1)-surfaces of coinage metals. For these systems the coupling is well understood [21], however, the VLs have been only published for P2O and P4O thin films on Ag(1 1 1) [74].

Experimental and computational details

COHON and PYTON were synthesized according to [75]. P2O and P4O were purchased from Sigma Aldrich. Metal single crystals were cleaned by repeated cycles of annealing (up to 550 °C) and Ar-ion sputtering. Organic materials were sublimed on the clean surfaces from resistively heated sources. The nominal mass-thickness of the organic layers was monitored with a quartz crystal microbalance. During deposition of COMs and during all measurements the substrates were kept at room temperature. Photoelectron spectroscopy experiments were performed at the endstation SurICat (beamline

PM4) [76] at the synchrotron light source BESSY II (Berlin, Germany). Spectra were collected with a hemispherical electron energy analyzer (Scienta SES 100) using an excitation photon energy of 35 eV for UPS and 620 eV for XPS. The secondary electron cutoff (SECO) spectra were obtained with the samples biased at -10 V in order to compensate for the analyzer's work function. The experimental setup consists of interconnected sample preparation (base pressure $<7 \times 10^{-9}$ mbar) and analysis (base pressure 1×10^{-10} mbar) chambers. The error of all energy values reported here is estimated to be ± 0.05 eV.

The XSW experiments were done in back-reflection geometry at beamline ID32 of the ESRF (Grenoble, France) [77] with the hemispherical electron analyzer (PERKIN Elmer PHI model) mounted at an angle of 45° relative to the incoming x-ray beam at a base pressure of 3×10^{-10} mbar. COHON and PYTON (nominal thickness: 2 Å) were evaporated directly in the analysis chamber. Analysis of the XSW data was performed using the software package *dare* (developed by JZ). The errors of the average bonding distances are estimated to be ± 0.05 Å and the error of the coherent fractions to ± 0.10 . The non-dipole contributions have been taken into account according to [78, 79].

Density functional theory calculations were performed using the *Fritz-Haber-Institute ab initio simulation* package (FHI-aims) [80] using the converged 'tight' default settings. We employed the PBE functional [81]. To account for long-range van-der-Waals interactions, the functional was augmented by the Tkatchenko–Scheffler scheme, which employs a density dependent C_6/r^6 correction [82]. For Cu, the van-der-Waals parameters were obtained by combining the free atom parameters with the Zaremba–Kohn–Lifshitz theory [83]. For molecules adsorbed on coinage metals, this method has been shown to yield both accurate adsorption geometries [83–85] and adequate interface dipoles, for which computationally more expensive hybrid functionals yield only minor improvements [20]. COHON and PYTON were put on 5-layer slabs of Cu and the top two metal layers were fully relaxed. In lieu of an experimentally determined unit cell, a $5 \times 3\sqrt{3}$ cell was assumed with only one molecule per supercell (see supporting information), including 50 Å of vacuum above the surface. Such a unit cell corresponds to a moderate packing density in which the interactions between the individual molecules are sufficiently small to avoid artifacts from incorrect packing. The reciprocal space was sampled by a $3 \times 3 \times 1$ Monkhorst–Pack [86] grid. All states were broadened using a Gaussian occupation scheme with 0.1 eV broadening. Electrostatic interactions between periodic replicas of the unit cells to the surface were prevented using a self-consistent dipole correction.

Evolution of the VL

A common descriptor for the energy-level alignment at organic-inorganic interfaces is the so-called 'slope parameter' S derived from plots of the adsorbate VL versus the substrate ϕ . In case of Fermi-level pinning S is 0, while for

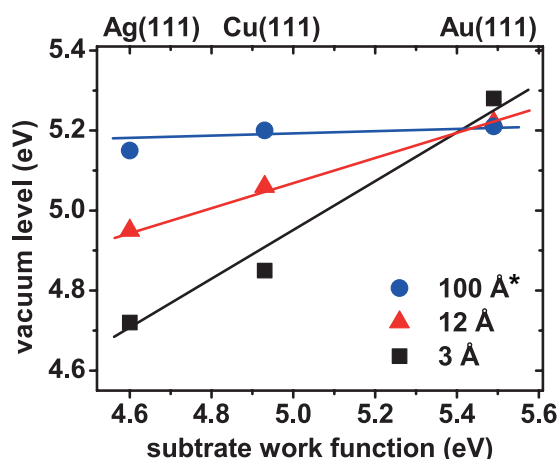


Figure 1. Vacuum level relative to the Fermi-level of COHON thin films with different nominal thicknesses as function of the substrate work function. The lines are guides to the eye. *On Ag(1 1 1) this data point was measured for a nominal COHON thickness of 50 Å.

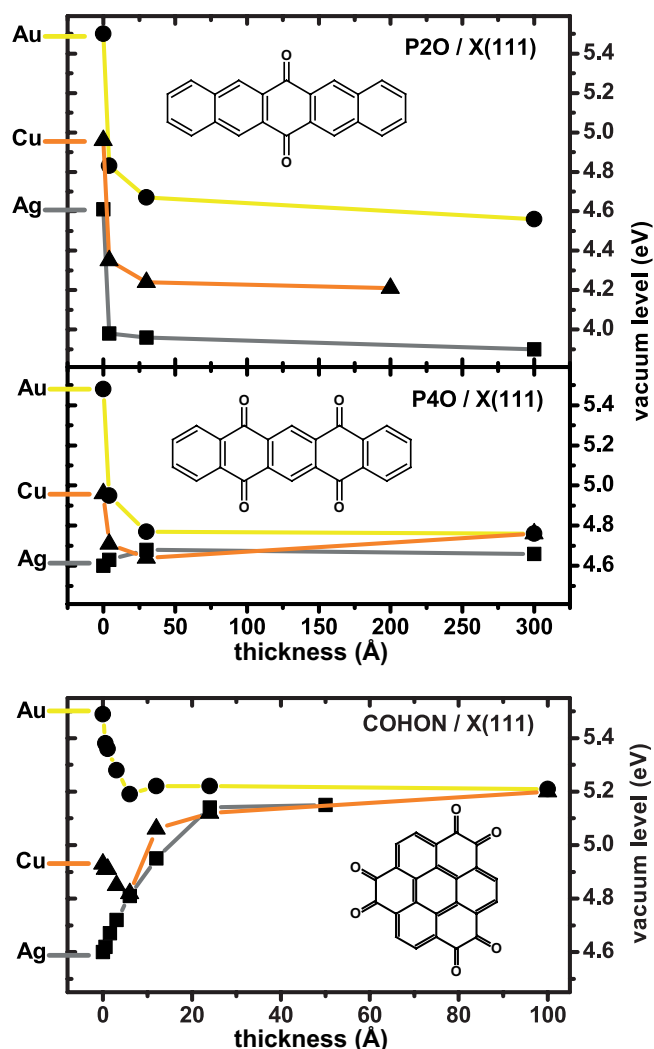


Figure 2. Thickness-dependent evolution of the VL of P2O, P4O and COHON on Au(1 1 1), Ag(1 1 1) and Cu(1 1 1), respectively. The initial work functions of the clean substrates were 5.50 eV, 4.60 eV and 4.95 eV, respectively. All values are taken from the SECO positions of UPS measurements. The insets show the chemical structures of the COMs.

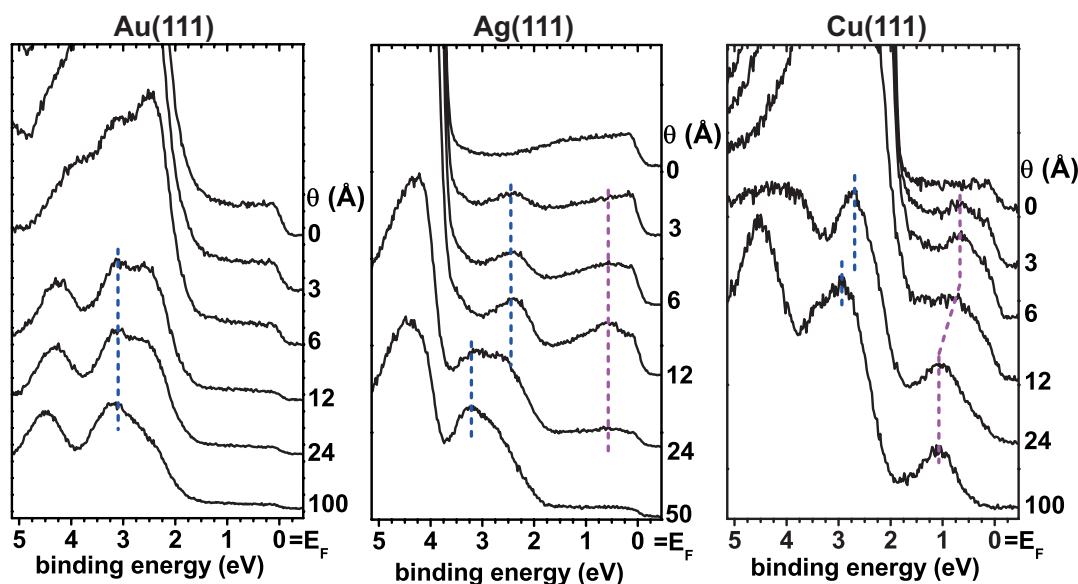


Figure 3. Valence electron spectra of COHON on X(111). θ denotes the nominal thickness and E_F the Fermi-energy. All spectra are collected at an emission angle of 45° . Vertical lines are guides to the eye and indicate the evolution of the HOMO and the former LUMO derived peaks.

the VL-controlled energy-level alignment S is 1 [7, 11, 87]. Figure 1 shows the vacuum levels with respect to the substrate Fermi-level (as deduced from the UPS SECOs) for COHON thin films with different nominal thicknesses on the (111)-surfaces of coinage metals. Interestingly, with increasing thickness S changes from ≈ 1 to ≈ 0 , i.e. from a VL to a Fermi-level controlled situation.

To understand this behavior, we start with a discussion of the VLs of P2O and P4O thin films with increasing nominal thickness on the same surfaces (figure 2). In the contact layer to clean metals, vacuum-sublimed COMs usually adopt a face-on (flat-lying) orientation. Then a nominal thickness of around 4 Å corresponds to a wetting layer [3, 24, 72, 88]. Indeed, P2O and P4O have in common that their VLs decrease up to a nominal thickness of 4 Å. Due to the coarse deposition step-width and island growth of P2O and P4O on the surfaces under investigation [21], a precise assignment of nominal monolayer coverage is not possible. Nevertheless, the VL stays almost constant for larger thicknesses on almost all substrates. The only exception is P4O on Ag, which exhibits a small increase in the VL upon monolayer formation.

For P2O the decrease of the VL is between -0.6 eV and -0.7 eV on all substrates and the different work functions of clean metals ($\phi_{\text{Au}} = 5.50$ eV; $\phi_{\text{Ag}} = 4.60$ eV; $\phi_{\text{Cu}} = 4.95$ eV) are still reflected in the VLs of P2O multilayers. The energy-level alignment at these interfaces is thus VL-controlled. On the other hand, P4O multilayers (with a nominal thickness of 300 Å) have almost the same VL (4.75 eV on Au and Cu and 4.65 eV on Ag) and are Fermi-level pinned.

To understand this contrasting behavior of these rather similar pentacene carbonyl-derivatives, it is helpful to take the contributions to Δ VL into account. The coupling between PxO and Au, and P2O and Ag is weak [21] and the decrease in the VLs can be mainly ascribed to the so-called push-back effect by COM adsorption [6, 89, 90], i.e. the reduction of ϕ by pushing back some of the electron density spilling

out into the vacuum at clean metal surfaces [91]. On the (111)-surfaces of coinage metals the push-back effect leads to Δ VLs of typically 0.5 eV–1.0 eV [92–94], which is line with the observed VL-shifts. P4O on Ag and PxO on Cu are strongly coupled involving CTC formation and a (partial) filling of the former LUMO [21]. In these cases, a net electron transfer into the molecules in the monolayer can be expected, resulting in an additional interface dipole, which counteracts the push-back effect [15, 95, 96]. One driving force for charge transfer is surface-induced aromatic stabilization [97, 98], as for P2O and P4O in the gas phase the conjugation does not extend over the entire molecule but is broken by the carbonyl groups. By CTC formation and hybridization with the surface, the π -system can extend over almost the entire molecule [21].

For COHON on Au (figure 2) the VL decreases by 0.30 eV upon deposition of nominally 6 Å COHON and stays constant for larger thicknesses. On Ag the VL increases up to a nominal COHON thickness of 24 Å, which is clearly beyond monolayer coverage for face-on COHON. A similar behavior is observed on Cu. However, here the VL initially *decreases* up to a nominal thickness of 6 Å. This unusual trend of the VLs on Ag and Cu leads to the thickness-dependent transition from VL-controlled to Fermi-level pinned (figure 1). It can have several reasons: (i) a low sticking coefficient of COHON on Ag and Cu [99, 100], (ii) pronounced island growth and/or dewetting [101–103], (iii) an edge-on orientation [104] or (iv) a reorientation from face-on to edge-on [30, 105]. As detailed below, the most plausible scenarios are edge-on COHON on Ag and a reorientation from face-on to edge-on COHON on Cu.

Valence electronic structure

We now turn to the valence electron region spectra of COHON on X(111) measured by UPS (figure 3). On Au, the absence of molecule-derived features close to E_F for low thicknesses is

indicative of weak interfacial interaction. For multilayer coverage (in this case a nominal thickness of 100 Å) the onset of the HOMO-derived peak is found at 1.85 eV binding energy (BE). For lower thicknesses, the position of this peak cannot be determined as it is masked by the photoemission intensity from Au d-bands in the BE range of around 1.5 eV–4.5 eV.

For low thicknesses on Ag two adsorbate derived features, centered at 0.60 eV BE and 2.40 eV BE, can be observed. They are most pronounced for a nominal thickness of 12 Å, which is around monolayer coverage for edge-on COHON, and their intensity decreases with increasing thickness. This behavior is similar to that of other COMs on metal surfaces with CTC formation [21, 96, 106, 107]. In analogy, the peak at lower BE can be assigned to the former LUMO and the one at higher BE to the relaxed HOMO of COHON in immediate contact with Ag. The HOMO of neutral multilayers (visible for nominal thicknesses of 24 Å and 50 Å) is centered at 3.20 eV BE and its onset is at 1.85 eV BE.

Also on Cu an interface state appears due to CTC formation. We attribute the shift of the peak maximum from 0.65 eV BE (6 Å thickness) to 1.05 eV BE (100 Å thickness) to a reorientation from face-on to edge-on: due to a cooperative impact of intramolecular dipole moments, EA (and IE) of molecular thin films depend on the molecular orientation [30, 108–110]. For COHON a transition from face-on to edge-on leads to an increase of EA and thus to a shift of the former LUMO derived UPS-peak to higher BE. A similar shift due to reorientation has been observed for NO₂-PYTON on Ag(111) [30]. The interface state is still visible for a nominal thickness of 100 Å, which is clearly beyond monolayer coverage even for edge-on molecules. The Fermi-edge is, however, not visible for nominal thicknesses larger than 24 Å. This points to pronounced island growth on a wetting layer of edge-on COHON. As on Au and Ag, the onset of the HOMO-derived peak of neutral multilayers is found at 1.85 eV BE and the IE (determined by this onset and the VL) is 7.05 eV.

Interfacial chemical interaction

The UPS data could establish that the interaction between COHON and Au is weak and the interaction with Ag and Cu is more chemisorptive and involves a larger net electron transfer. The discussion of the C1s and O1s core-level spectra gives more detailed insight into the chemical interaction at these interfaces. Figure 4 shows fits to spectra dominated by monolayer features (nominally 6 Å on all substrates) and multilayer features (100 Å on Au and Cu and 50 Å on Ag), respectively. The full data set of thickness-dependent spectra is included in the supporting information.

On Au, the C1s derived peak is split into two components which are (for monolayer coverage) centered at 284.25 eV BE and 286.85 eV BE, respectively. From their energetic positions and intensity ratio, these peaks can be assigned to aromatic carbons (lower BE) and carbonyl carbons (higher BE), respectively. For multilayer coverage the C1s peaks are centered at 284.85 eV BE and 287.15 eV BE. Such almost rigid

shifts can be mainly ascribed to the final state screening effect [29, 111, 112] and are typical for weakly interacting systems. The multilayer C1s spectra of COHON on Ag and Cu exhibits two pronounced peaks at similar energetic positions as on Au, which can, again, be assigned to aromatic and carbonyl carbons. However, for lower thicknesses the carbonyl–carbon derived peaks exhibit strong chemical shifts (by 1.9 eV on Ag and by 1.8 eV on Cu) towards lower BE, i.e. towards the aromatic carbon peak. This is fully in line with surface-induced aromatic stabilization of COHON on Ag and Cu, as in the charged monolayer all carbon atoms acquire a more aromatic character [21].

For monolayer coverages of COHON on Au, the O1s-derived peak is centered at 531.10 eV BE and exhibits a shoulder at the low BE side. Upon increasing thickness, the main peak shifts to higher BE (final value: 531.50 eV BE) and the relative intensity of the shoulder decreases. The shift can, again, mainly be attributed to the screening effect. The shoulder (with a comparably low intensity) can be associated with a weak interaction between COHON and Au. An interaction beyond physisorption has been also suggested for COHON on polycrystalline Au [113]. The situation is strikingly different on Ag and Cu. In both cases, the O1s derived peak shows strong chemical shifts between mono- and multilayer (1.7 eV on Ag and 0.8 eV on Cu). This hints towards CTC formation between COHON molecules in the contact layer to Ag and Cu and suggests neutral multilayers.

Bonding distances

Having described the electronic structure, we now turn to the impact of CTC formation on the bonding distances, which we discuss using the example of COHON on Cu. Employing the XSW technique to (sub)monolayers of lying organic adsorbates on metallic single crystalline substrates allows determining element-specific averaged bonding distances with high precision [72, 114, 115]. The photoelectron yield (Y_p), i.e. the adsorbate core-level XPS intensity, is measured as function of excitation energy around the Bragg-energy. This allows determining the coherent fraction (f_H), which is a measure for the degree of order of the adsorbate, and the coherent position (P_H). For an edge-on orientation the individual carbon atoms of one molecule have rather different vertical adsorption distances resulting in f_H close to 0. In that case an averaged P_H cannot be determined. Basically, i.e. without going into the details of non-dipole corrections, the photoelectron yield is given by [116, 117]:

$$Y_p = 1 + R + \sqrt{R}f_H \cos(\nu - 2\pi P_H) \quad (1)$$

with R being the reflectivity and ν the relative phase of the interfering wave fields. The element specific average adsorption distance (d_H) can then be determined by:

$$d_H = d_0(n + P_H) \quad (2)$$

with n being an integer and $d_0 = 2.09$ Å the lattice plane spacing of the (111) reflection of Cu. Figure 5 includes the Y_p

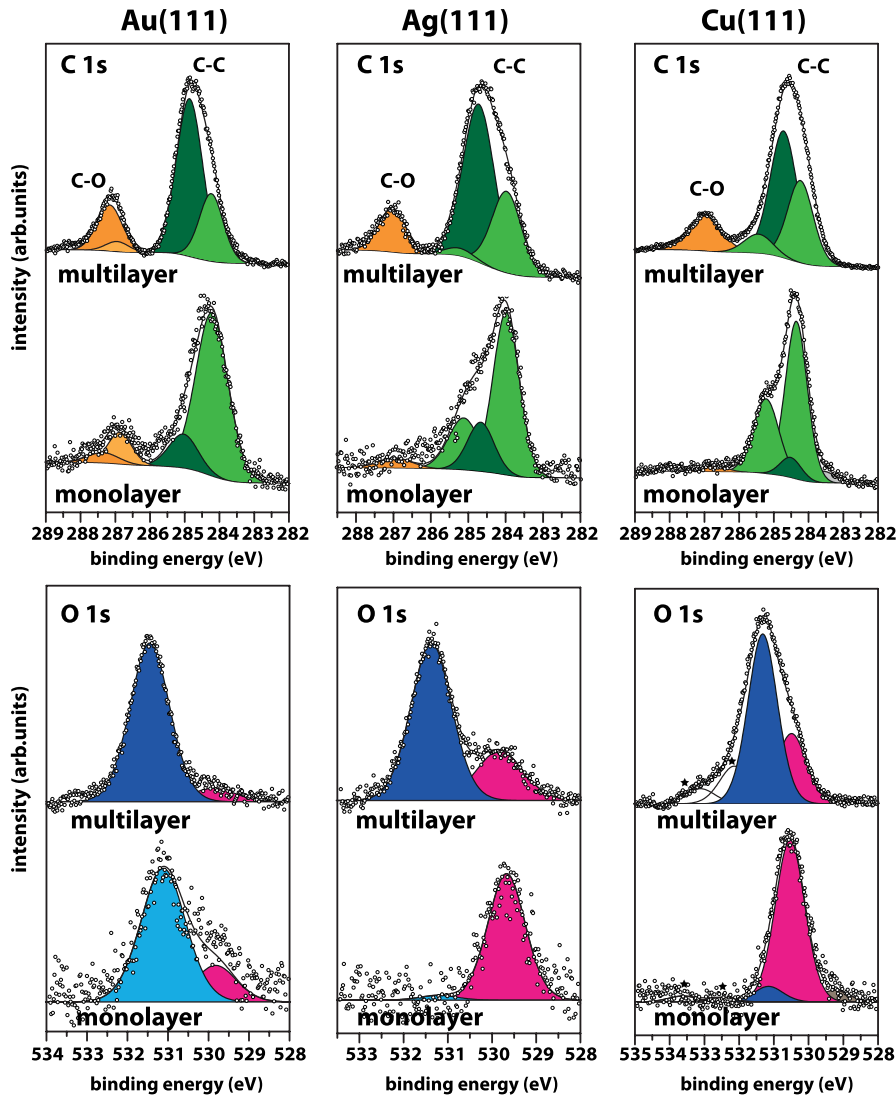


Figure 4. C1s and O1s spectra of COHON on the three investigated surfaces. In each plot, spectra for nominal monolayer (bottom) and multilayer (top) coverage and corresponding least mean square fits are displayed. Due to Stranski–Krastanov growth, most spectra include monolayer as well as multilayer contributions; the latter are displayed in darker colors. In the C1s spectra, contributions of aromatic carbons (C–C) are displayed in green and carbonyl carbons (C–O) in orange. In the O1s spectra, blue areas stem from oxygen atoms in neutral molecules and pink areas from those in charged molecules. Stars mark shake-up excitations.

data with the fits and the parameters f_H , P_H as well as a sketch of the adsorption geometries for COHON on Cu. They are in excellent agreement with the bonding distances computed with DFT (*vide infra*).

The coherent fractions are in the range of 0.30–0.50, which points—for this particular experimental setup [118]—to rather flat lying molecules [72, 89, 119]. The nominal thickness for XSW measurements was 2 Å and for this thickness a face-on orientation has been also suggested by the UPS results. The finding of coherent fractions for carbons being smaller than those for oxygens can be explained by the experimental averaging over all carbon atoms in the respective molecules. The experimentally determined molecular distortion (~ 0.30 Å) is virtually the same distortion as for P2O and P4O on the same substrate [21]. There, the out-of-plane bending of the C–O bond was explained by the tendency of this bond towards sp^3 -hybridization upon CTC formation [21].

Charge rearrangements upon contact formation

For a better understanding of VL-shifts by organic/inorganic contact formation, the calculated total change of the VL, i.e. the interface dipole ΔVL , is often split into two components: a contribution due to the molecular dipole perpendicular to the surface (which can be influenced by geometry rearrangements upon adsorption), ΔVL_{mol} , and the bond dipole, ΔVL_{bond} :

$$\Delta VL = \Delta VL_{\text{mol}} + \Delta VL_{\text{bond}}. \quad (3)$$

ΔVL_{bond} represents the shift in the electrostatic potential due to adsorption-induced charge-rearrangements $\Delta\rho$, which are calculated as the difference of the total electron density of the combined metal/organic interface (ρ^{sys}) and the non-interacting densities of metal (ρ^{Metal}) and monolayer ($\rho^{\text{Monolayer}}$) on their own (where the geometries of the sub-systems are fixed at those calculated for the interacting case):

$$\Delta\rho = \rho^{\text{sys}} - (\rho^{\text{metal}} + \rho^{\text{monolayer}}). \quad (4)$$

From $\Delta\rho$, $\Delta\text{VL}_{\text{bond}}$ is then obtained by solving the Poisson equation. At this point it is important to remember that for molecules that undergo charge-transfer reactions with the surface, $\Delta\text{VL}_{\text{mol}}$ and $\Delta\text{VL}_{\text{bond}}$ are *not* independent. Rather, any error in the description of the bending is made up for by a change in charge-transfer. This makes ΔVL , which is the experimental observable, a very robust quantity [120].

In the gas phase COHON is planar. Thus, all contributions to $\Delta\text{VL}_{\text{mol}}$ are due to adsorption-induced conformational changes. The bending of COHON (see figure 5), induces a *decrease* in the VL of -0.56 eV . The molecular dipoles $\Delta\text{VL}_{\text{mol}}$ are partially compensated by the charge-transfer from the metal to the molecule [120], which leads to $\Delta\text{VL}_{\text{bond}}$ of $+0.54\text{ eV}$ and, eventually, to ΔVL of -0.02 eV for COHON on Cu. On first sight, this seems to be at variance with the measured ΔVL ($+0.27\text{ eV}$). However, the calculations were performed for a monolayer of face-on COHON (supercell in the supporting information) and also the experimentally determined VL decreases slightly up to a nominal COHON thickness of 6 \AA (figure 2). The increase in the VL sets in only for larger thicknesses. This suggests that it is not caused by a face-on COHON monolayer. In analogy to the situation in NO_2 -PYTON we hypothesize that the increase in VL can be ascribed to the reorientation of COHON, which is not considered in the calculations. To gain microscopic insight into what happens for the flat-lying layer, figure 6 displays the calculated charge rearrangements upon contact formation for COHON on Cu averaged over the xy -plane (left panel) and in 3D (right panel). A characteristic double-peak structure above and below the molecule is found, which is indicative of a filling of a previously unoccupied π -orbital.

Discussion and conclusion

Multilayers of COHON on all three investigated substrates are Fermi-level pinned: they show identical onsets of the HOMO-derived peak (at 1.85 eV BE) as well as identical VLs of 5.20 eV and, consequently, also the same IE of 7.05 eV (figure 7). Based on the thickness-dependent VL evolution (figure 2) also P4O is Fermi-level pinned on all substrates, whereas P2O is VL controlled.

In order to understand the energy-level alignment mechanisms in more detail, first some pitfalls for extracting relevant parameters from UP spectra will be discussed. UPS (and XPS) measurements cannot give conclusive proof about the orientation (face-on or edge-on). Moreover, due to the tendency for Stranski–Krastanov or island growth for all investigated systems, pure ‘monolayer’ or ‘multilayer’ spectra are often not accessible. Special care has to be taken for the correct assignment of the VL as, in case of a laterally non-uniform VL directly above the sample, the VL measured by UPS is in between the limiting VL values [121]. Island growth can, thus, create the impression of a coverage-dependent shift of the VL. This also impacts the correct assignment of IEs [122–124], which is further complicated by dominating photoemission intensity from metal d-bands for low molecular coverage. For

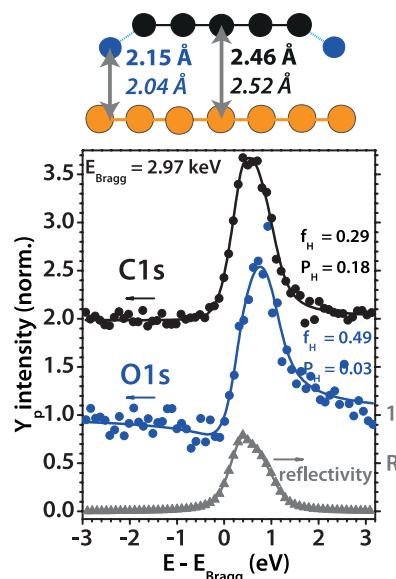


Figure 5. Photoelectron yield Y_p of C1s and O1s core levels of COHON on Cu(1 1 1) as well as reflectivity R as function of energy relative to the Bragg energy $E_{\text{Bragg}} = 2.97\text{ keV}$. Symbols correspond to experimental data and lines to least mean square fits, from which the coherent fractions (f_H) and the coherent positions (P_H) are determined. Curves are vertically shifted for the sake of clarity. On top schematics (not to scale) of the bonding geometry and the averaged bonding distances for carbon (black) and oxygen (blue) atoms from XSW experiments (bold) and DFT calculations (semibold italic) are given.

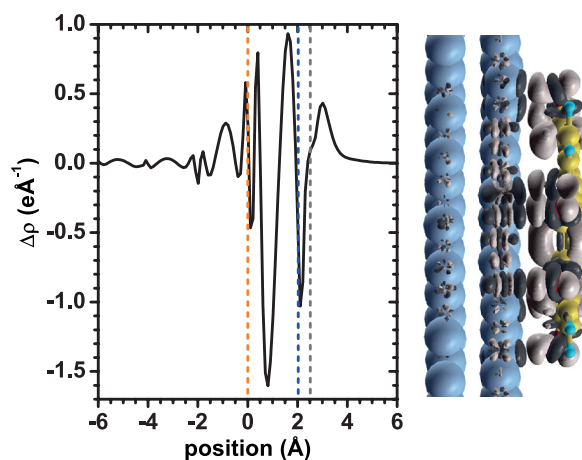


Figure 6. Left panel: plane-integrated charge rearrangement ($\Delta\rho$) perpendicular to the surface upon formation of the organic–metal interface for COHON on Cu(1 1 1). The dashed lines mark the top metal layer (set to zero) and the averaged DFT calculated bonding distances of carbon and oxygen atoms. Right panel: electron accumulation (light gray) and electron depletion (dark gray) upon contact formation.

example, the HOMO positions of a monolayer of COHON on Au and on Cu cannot be extracted from UPS data (figure 3) and are consequently just estimated in the energy-level diagram (figure 7). Moreover, due to experimental difficulties IPES experiments at organic–metal interfaces are not routinely performed [6, 125–128] and LUMO positions are often approximated by the optical gap plus an (estimated) exciton BE [129]. Overall, the most reliable experimentally

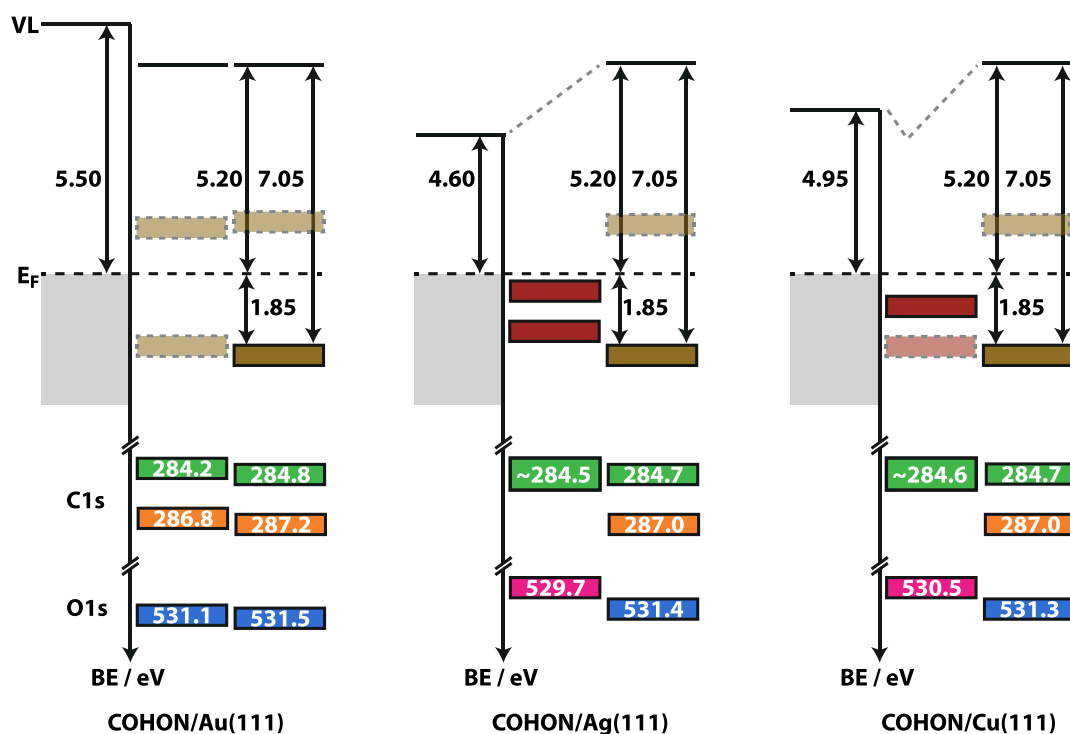


Figure 7. Schematic energy-level diagrams for COHON on X(111). In each case, on the left the respective metal substrate with its work function and Fermi-level (E_F) is displayed. Each middle panel corresponds to a COHON monolayer and reports the position of the (former) LUMO, the HOMO position and the energetic position of C1s and O1s core-levels. In addition, for multilayer coverage (right panels) also the position of the VL, the onset of the HOMO and the resulting IE values are displayed. All energies are given in eV, energy axes are not to scale. Levels, which were not directly measured, are indicated by dotted lines. This applies in particular to the VL for monolayer coverage and the LUMO position in multilayers, which are estimated by the optical gap (3.30 eV, measured in solution) [70].

accessible parameters for the discussion of energy-level alignment mechanisms at organic–metal interfaces are, thus, multilayer IE and VL (figure 7).

With the available data for COHON, the energy-level alignment on Ag and Cu can be well explained: in both cases the coupling is strong and involves CTC formation. Consequently, COHON thin films on both substrates are Fermi-level pinned and have the same VL. Due to the reorientation of COHON on Cu, Fermi-level pinning is fully effective only for a relatively large thickness (figure 1). Seemingly, the reasoning of strong coupling cannot be applied to COHON on Au, which, based on UPS and XPS, only involves weak interaction. However, the small shoulder at the low BE side of the O1s-derived peak (figure 4) points to interaction beyond physisorption. Moreover, also the relatively small ΔVL (0.30 eV) points to organic–metal charge transfer counteracting push-back. The associated additional density of occupied states by partial filling of the COHON LUMO could be simply rather small and beyond the detection limit of conventional UPS [130–132].

In conclusion, for sufficiently high nominal thicknesses, thin films of COHON and P4O on the (111)-surfaces of coinage metals are found to be Fermi-level pinned irrespective of the wide range of the work functions of the pristine metal substrates. This, in fact, applies to the weakly interacting interface on Au and to the strongly chemisorptive interfaces on Ag and Cu and is, thus, independent of the interaction strength. The energy-level alignment of P2O, on the other hand, is vacuum-level controlled on the same surfaces. The VL of COHON thin films on the (111)-surfaces of coinage

metals (5.20 eV) is much further from the Fermi-level than that of P4O or PYTON thin films (4.60 or 4.70 eV). COHON covered metals are, thus, highly promising as hole injection electrodes for organic electronics devices.

Acknowledgments

The authors thank Georg Heimel for many inspiring discussions and the synchrotron radiation facilities ESRF and BESSY II for providing beamtime. This work was financially supported in part by the National Key R&D Program of China (Grant No. 2017YFA0205002), the 111 Project of the Chinese State Administration of Foreign Experts Affairs, the Collaborative Innovation Center of Suzhou Nano Science & Technology (NANO-CIC), the Soochow University-Western University Joint Center for Synchrotron Radiation Research and the DFG. OTH gratefully acknowledges support by the Austrian Science Fund (FWF): P27868-N36 and P28631-N36. IS acknowledges support of the Natural Sciences and Engineering Research Council of Canada (NSERC) (funding reference number RGPIN-2018-05092) and by Concordia University. The computational results presented have been achieved in part using the Vienna Scientific Cluster (VSC).

Supporting information

The supporting information includes additional UP and XP spectra of COHON on X(111), UP and XP spectra of PYTON

on Cu(1 1 1), supercells for COHON on Cu(1 1 1) and PYTON on Cu(1 1 1), the results from XSW measurements of PYTON on Cu(1 1 1) and DFT-modeled charge rearrangements for PYTON on Cu(1 1 1).

ORCID iDs

Oliver T Hofmann  <https://orcid.org/0000-0002-2120-3259>
 Frank Schreiber  <https://orcid.org/0000-0003-3659-6718>
 Norbert Koch  <https://orcid.org/0000-0002-6042-6447>
 Egbert Zojer  <https://orcid.org/0000-0002-6502-1721>
 Steffen Duhm  <https://orcid.org/0000-0002-5099-5929>

References

- [1] Hwang J, Wan A and Kahn A 2009 *Mater. Sci. Eng. R* **64** 1
- [2] Zhou Y et al 2012 *Science* **336** 327
- [3] Klappenberger F 2014 *Prog. Surf. Sci.* **89** 1
- [4] Otero R, Vázquez de Parga A and Gallego J 2017 *Surf. Sci. Rep.* **72** 105
- [5] Han G, Yi Y and Shuai Z 2018 *Adv. Energy Mater.* **8** 1702743
- [6] Kahn A, Koch N and Gao W Y 2003 *J. Poly. Sci. B* **41** 2529
- [7] Braun S, Salaneck W R and Fahlman M 2009 *Adv. Mater.* **21** 1450
- [8] Ishii H, Sugiyama K, Ito E and Seki K 1999 *Adv. Mater.* **11** 605
- [9] Ley L, Smets Y, Pakes C I and Ristein J 2013 *Adv. Funct. Mater.* **23** 794
- [10] Oehzelt M, Koch N and Heimel G 2014 *Nat. Commun.* **5** 4174
- [11] Yang J-P, Bussolotti F, Kera S and Ueno N 2017 *J. Phys. D: Appl. Phys.* **50** 423002
- [12] Khoshkhoo M S, Peisert H, Chasse T and Scheele M 2017 *Org. Electron.* **49** 249
- [13] Blyholder G 1964 *J. Phys. Chem.* **68** 2772
- [14] Tautz F S 2007 *Prog. Surf. Sci.* **82** 479
- [15] Romaner L, Heimel G, Brédas J-L, Gerlach A, Schreiber F, Johnson R L, Zegenhagen J, Duhm S, Koch N and Zojer E 2007 *Phys. Rev. Lett.* **99** 256801
- [16] Tseng T-C et al 2010 *Nat. Chem.* **2** 374
- [17] Vitali L, Levita G, Ohmann R, Comisso A, De Vita A and Kern K 2010 *Nat. Mater.* **9** 320
- [18] Häming M, Schöll A, Umbach E and Reinert F 2012 *Phys. Rev. B* **85** 235132
- [19] Liu W, Filimonov S N, Carrasco J and Tkatchenko A 2013 *Nat. Commun.* **4** 2569
- [20] Hofmann O T, Atalla V, Moll N, Rinke P and Scheffler M 2013 *New J. Phys.* **15** 123028
- [21] Heimel G et al 2013 *Nat. Chem.* **5** 187
- [22] Stadtmüller B et al 2014 *Nat. Commun.* **5** 3685
- [23] Willenbockel M, Lüftner D, Stadtmüller B, Koller G, Kumpf C, Soubatch S, Puschnig P, Ramsey M G and Tautz F S 2015 *Phys. Chem. Chem. Phys.* **17** 1530
- [24] Goiri E, Borghetti P, El-Sayed A, Ortega J E and de Oteyza D G 2016 *Adv. Mater.* **28** 1340
- [25] Yonezawa K, Suda Y, Yanagisawa S, Hosokai T, Kato K, Yamaguchi T, Yoshida H, Ueno N and Kera S 2016 *Appl. Phys. Express* **9** 045201
- [26] Kröger I, Stadtmüller B and Kumpf C 2016 *New J. Phys.* **18** 113022
- [27] Armbrust N, Schiller F, Güdde J and Höfer U 2017 *Sci. Rep.* **7** 46561
- [28] Ugolotti A, Harivyasi S S, Baby A, Dominguez M, Pinardi A L, Lopez M F, Martin-Gago J A, Fratesi G, Floreano L and Brivio G P 2017 *J. Phys. Chem. C* **121** 22797
- [29] Franco-Cañellas A, Wang Q, Broch K, Duncan D A, Thakur P K, Liu L, Kera S, Gerlach A, Duhm S and Schreiber F 2017 *Phys. Rev. Mater.* **1** 013001
- [30] Hofmann O T et al 2017 *J. Phys. Chem. C* **121** 24657
- [31] Zamborlini G et al 2017 *Nat. Commun.* **8** 335
- [32] Lerch A, Zimmermann J E, Namgalies A, Stallberg K and Höfer U 2018 *J. Phys.: Condens. Matter* **30** 494001
- [33] Blowey P J, Velari S, Rochford L A, Duncan D A, Warr D A, Lee T-L, De Vita A, Costantini G and Woodruff D P 2018 *Nanoscale* **10** 14984
- [34] Maughan B, Eads C N, Zahl P and Monti O L A 2018 *Phys. Rev. B* **98** 155106
- [35] Zaitsev N L, Jakob P and Tonner R 2018 *J. Phys.: Condens. Matter* **30** 354001
- [36] Winkler S, Xin Q, Li C, Kera S, Müllen K, Ueno N, Koch N and Duhm S 2019 *Electron. Struct.* **1** 015007
- [37] Tong Y, Fuhr J D, Martiarena M L, Oughaddou H, Enriquez H, Nicolas F, Chaouchi K, Kubsy S and Bendounan A 2019 *J. Phys. Chem. C* **123** 379
- [38] Liu Z-F, Egger D A, Refaely-Abramson S, Kronik L and Neaton J B 2017 *J. Chem. Phys.* **146** 092326
- [39] Maurer R J, Ruiz V G, Camarillo-Cisneros J, Liu W, Ferri N, Reuter K and Tkatchenko A 2016 *Prog. Surf. Sci.* **91** 72
- [40] Packwood D M, Han P and Hitosugi T 2017 *Nat. Commun.* **8** 14463
- [41] Obersteiner V, Scherbela M, Hörmann L, Wegner D and Hofmann O T 2017 *Nano Lett.* **17** 4453
- [42] Koch N and Vollmer A 2006 *Appl. Phys. Lett.* **89** 162107
- [43] Braun S and Salaneck W R 2007 *Chem. Phys. Lett.* **438** 259
- [44] Derry G N, Kern M E and Worth E H 2015 *J. Vac. Sci. Technol. A* **33** 060801
- [45] Manandhar K and Parkinson B A 2010 *J. Phys. Chem. C* **114** 15394
- [46] Lu M-C, Wang R-B, Yang A and Duhm S 2016 *J. Phys.: Condens. Matter* **28** 094005
- [47] Koch N, Vollmer A, Duhm S, Sakamoto Y and Suzuki T 2007 *Adv. Mater.* **19** 112
- [48] Duhm S et al 2010 *Phys. Rev. B* **81** 045418
- [49] Glowatzki H, Heimel G, Vollmer A, Wong S L, Huang H, Chen W, Wee A T S, Rabe J P and Koch N 2012 *J. Phys. Chem. C* **116** 7726
- [50] Duhm S, Gerlach A, Salzmann I, Bröker B, Johnson R L, Schreiber F and Koch N 2008 *Org. Electron.* **9** 111
- [51] Zu F, Amsalem P, Ralaifarisoa M, Schultz T, Schlesinger R and Koch N 2017 *ACS Appl. Mater. Interfaces* **9** 41546
- [52] Yang J-P, Bussolotti F, Li Y-Q, Zeng X-H, Kera S, Tang J-X and Ueno N 2015 *Org. Electron.* **24** 120
- [53] Lee S, Lee J-H, Kim K H, Yoo S-J, Kim T G, Kim J W and Kim J-J 2012 *Org. Electron.* **13** 2346
- [54] Christodoulou C et al 2014 *J. Phys. Chem. C* **118** 4784
- [55] Kanai K, Akaike K, Koyasu K, Sakai K, Nishi T, Kamizuru Y, Nishi T, Ouchi Y and Seki K 2009 *Appl. Phys. A* **95** 309
- [56] Gao W and Kahn A 2001 *Appl. Phys. Lett.* **79** 4040
- [57] Zahn D R, Gavrila G N and Gorgoi M 2006 *Chem. Phys.* **325** 99
- [58] Wang R-B, Wang Q-K, Xie H-J, Xu L-H, Duhm S, Li Y-Q and Tang J-X 2014 *ACS Appl. Mater. Interfaces* **6** 15604
- [59] Najafabadi E, Knauer K A, Haske W and Kippelen B 2013 *Org. Electron.* **14** 1271
- [60] Liao L-S, Slusarek W-K, Hatwar T-K, Ricks M-L and Comfort D-L 2008 *Adv. Mater.* **20** 324
- [61] Lee S, Lee J-H, Lee J-H and Kim J-J 2012 *Adv. Funct. Mater.* **22** 855
- [62] Jacobs I E and Moulé A J 2017 *Adv. Mater.* **29** 1703063
- [63] Li J, Rochester C W, Jacobs I E, Friedrich S, Stroeve P, Riede M and Moulé A J 2015 *ACS Appl. Mater. Interfaces* **7** 28420

- [64] Zhang L, Zu F S, Deng Y L, Igbari F, Wang Z K and Liao L S 2015 *ACS Appl. Mater. Interfaces* **7** 11965
- [65] Amsalem P, Wilke A, Frisch J, Niederhausen J, Vollmer A, Rieger R, Müllen K, Rabe J P and Koch N 2011 *J. Appl. Phys.* **110** 113709
- [66] Bruder I, Watanabe S, Qu J, Müller I B, Kopecek R, Hwang J, Weis J and Langer N 2010 *Org. Electron.* **11** 589
- [67] Duhm S, Salzmann I, Bröker B, Glowatzki H, Johnson R L and Koch N 2009 *Appl. Phys. Lett.* **95** 093305
- [68] Tyagi P, Dalai M K, Suman C K, Tuli S and Srivastava R 2013 *RSC Adv.* **3** 24553
- [69] Futscher M H, Schultz T, Frisch J, Ralairisoa M, Metwalli E, Nardi M V, Müller-Buschbaum P and Koch N 2019 *J. Phys.: Condens. Matter* **31** 064002
- [70] Rieger R, Kastler M, Enkelmann V and Müllen K 2008 *Chem. Eur. J.* **14** 6322
- [71] Zegenhagen J 2013 *Springer Series in Surface Sciences* vol 51, ed G Bracco and B Holst (Berlin: Springer) pp 249–75
- [72] Gerlach A, Bürker C, Hosokai T and Schreiber F 2013 *The Molecule-Metal Interface* ed N Koch et al (New York: Wiley) pp 153–72
- [73] Hu J, Zhang D and Harris F W 2004 *J. Org. Chem.* **70** 707
- [74] Wang Q et al 2018 *J. Phys. Chem. C* **122** 9480
- [75] Watson M D, Fechtenkötter A and Müllen K 2001 *Chem. Rev.* **101** 1267
- [76] Vollmer A, Jurchescu O D, Arfaoui I, Salzmann I, Palstra T T M, Rudolf P, Niemax J, Pflaum J, Rabe J P and Koch N 2005 *Eur. Phys. J. E* **17** 339
- [77] Zegenhagen J, Detlefs B, Lee T-L, Thiess S, Isern H, Petit L, André L, Roy J, Mi Y Y and Joumard I 2010 *J. Electron Spectrosc. Relat. Phenom.* **178–9** 258
- [78] Schreiber F, Ritley K A, Vartanyants I A, Dosch H, Zegenhagen J and Cowie B C C 2001 *Surf. Sci.* **486** L519
- [79] Gerlach A, Schreiber F, Sellner S, Dosch H, Vartanyants I A, Cowie B C C, Lee T-L and Zegenhagen J 2005 *Phys. Rev. B* **71** 205425
- [80] Blum V, Gehrke R, Hanke F, Havu P, Havu V, Ren X, Reuter K and Scheffler M 2009 *Comput. Phys. Commun.* **180** 2175
- [81] Perdew J P, Burke K and Ernzerhof M 1996 *Phys. Rev. Lett.* **77** 3865
- [82] Tkatchenko A and Scheffler M 2009 *Phys. Rev. Lett.* **102** 073005
- [83] Ruiz V G, Liu W, Zojer E, Scheffler M and Tkatchenko A 2012 *Phys. Rev. Lett.* **108** 146103
- [84] Mercurio G et al 2013 *Phys. Rev. B* **88** 035421
- [85] Schuler B, Liu W, Tkatchenko A, Moll N, Meyer G, Mistry A, Fox D and Gross L 2013 *Phys. Rev. Lett.* **111** 106103
- [86] Monkhorst H J and Pack J D 1976 *Phys. Rev. B* **13** 5188
- [87] Koch N 2007 *Chem. Phys. Chem.* **8** 1438
- [88] Bouju X, Mattioli C, Franc G, Pujol A and Gourdon A 2017 *Chem. Rev.* **117** 1407
- [89] Duhm S, Bürker C, Hosokai T and Gerlach A 2015 *Springer Series in Materials Science* vol 209, ed H Ishii et al (Japan: Springer) pp 89–107
- [90] Bagus P S, Staemmler V and Wöll C 2002 *Phys. Rev. Lett.* **89** 096104
- [91] Smoluchowski R 1941 *Phys. Rev.* **60** 661
- [92] Ferri N, Ambrosetti A and Tkatchenko A 2017 *Phys. Rev. Mater.* **1** 026003
- [93] Toyoda K, Hamada I, Lee K, Yanagisawa S and Morikawa Y 2011 *J. Phys. Chem. C* **115** 5767
- [94] Toyoda K, Hamada I, Lee K, Yanagisawa S and Morikawa Y 2010 *J. Chem. Phys.* **132** 134703
- [95] Kawabe E, Yamane H, Sumii R, Koizumi K, Ouchi Y, Seki K and Kanai K 2008 *Org. Electron.* **9** 783
- [96] Koch N, Duhm S, Rabe J P, Vollmer A and Johnson R L 2005 *Phys. Rev. Lett.* **95** 237601
- [97] Marder S R, Beratan D N and Cheng L T 1991 *Science* **252** 103
- [98] Marder S R, Kippelen B, Jen A K-Y and Peyghambarian N 1997 *Nature* **388** 845
- [99] Witte G and Wöll C 2004 *J. Mater. Res.* **19** 1889
- [100] Duhm S, Glowatzki H, Cimpeanu V, Klankermayer J, Rabe J P, Johnson R L and Koch N 2006 *J. Phys. Chem. B* **110** 21069
- [101] Niederhausen J et al 2014 *J. Chem. Phys.* **140** 014705
- [102] Kowarik S 2017 *J. Phys.: Condens. Matter* **29** 043003
- [103] Winkler A 2016 *Surf. Sci.* **652** 367
- [104] Jones A O F, Chattopadhyay B, Geerts Y H and Resel R 2016 *Adv. Funct. Mater.* **26** 2233
- [105] Bröker B et al 2010 *Phys. Rev. Lett.* **104** 246805
- [106] Zou Y, Kilian L, Schöll A, Schmidt T, Fink R and Umbach E 2006 *Surf. Sci.* **600** 1240
- [107] Hollerer M, Lüftner D, Hurdax P, Ules T, Soubatch S, Tautz F S, Koller G, Puschnig P, Sterrer M and Ramsey M G 2017 *ACS Nano* **11** 6252
- [108] Heimel G, Salzmann I, Duhm S and Koch N 2011 *Chem. Mater.* **23** 359
- [109] Han W N et al 2013 *Appl. Phys. Lett.* **103** 253301
- [110] Duhm S, Heimel G, Salzmann I, Glowatzki H, Johnson R L, Vollmer A, Rabe J P and Koch N 2008 *Nat. Mater.* **7** 326
- [111] Hill I G, Mäkinen A J and Kafafi Z H 2000 *J. Appl. Phys.* **88** 889
- [112] Koch N 2008 *J. Phys.: Condens. Matter* **20** 184008
- [113] Medjanik K et al 2010 *Phys. Chem. Chem. Phys.* **12** 7184
- [114] Kera S, Hosokai T and Duhm S 2018 *J. Phys. Soc. Japan* **87** 061008
- [115] van Straaten G, Franke M, Bocquet F C, Tautz F S and Kumpf C 2018 *J. Electron Spectrosc. Relat. Phenom.* **222** 106
- [116] Zegenhagen J 1993 *Surf. Sci. Rep.* **18** 199
- [117] Woodruff D P 2005 *Rep. Prog. Phys.* **68** 743
- [118] Blowey P J, Rochford L A, Duncan D A, Warr D A, Lee T-L, Woodruff D P and Costantini G 2017 *Faraday Discuss.* **204** 97
- [119] Stadtmüller B, Schröder S and Kumpf C 2015 *J. Electron Spectrosc. Relat. Phenom.* **204** 80
- [120] Hofmann O T, Egger D A and Zojer E 2010 *Nano Lett.* **10** 4369
- [121] Schultz T, Lenz T, Kotadiya N, Heimel G, Glasser G, Berger R, Blom P W M, Amsalem P, de Leeuw D M and Koch N 2017 *Adv. Mater. Interfaces* **4** 1700324
- [122] Cahen D and Kahn A 2003 *Adv. Mater.* **15** 271
- [123] Wang Q, Xin Q, Wang R-B, Oehzelt M, Ueno N, Kera S and Duhm S 2017 *Phys. Status Solidi RRL* **11** 1700012
- [124] Schultz T, Amsalem P, Kotadiya N B, Lenz T, Blom P W M and Koch N 2018 *Phys. Status Solidi B* accepted (<https://doi.org/10.1002/pssb.201800299>)
- [125] Zahn D R T, Gavrila G N and Salvan G 2007 *Chem. Rev.* **107** 1161
- [126] Yoshida H 2015 *J. Electron Spectrosc. Relat. Phenom.* **204** 116
- [127] Yang A et al 2016 *Phys. Rev. B* **94** 155426
- [128] Yoshida H and Yoshizaki K 2015 *Org. Electron.* **20** 24
- [129] Djurovich P I, Mayo E I, Forrest S R and Thompson M E 2009 *Org. Electron.* **10** 515
- [130] Sato T, Kinjo H, Yamazaki J and Ishii H 2017 *Appl. Phys. Express* **10** 011602
- [131] Bussolotti F 2015 *J. Electron Spectrosc. Relat. Phenom.* **204** 29
- [132] Sueyoshi T, Fukagawa H, Ono M, Kera S and Ueno N 2009 *Appl. Phys. Lett.* **95** 183303